Deciphering The Power Reduction Due To Temperature In Commercial Photovoltaic Inverters

Geyciane Pinheiro de Lima, Diego Lucas de Carvalho Martinez, Alan Marques Leal de Sousa, João Pedro Carvalho Silveira, Pedro José dos Santos Neto, Tárcio André dos Santos Barros.

Universidade Estadual de Campinas (UNICAMP)/ Laboratório de Energia e Sistemas Fotovoltaicos Marcelo Villalva (LESF-MV), Campinas (Brazil)

Abstract

Commercial photovoltaic inverters operating in harsh conditions activate self-protection that reduces power, undermining energy yield and service life. Manufacturers' datasheets seldom disclose full derating curves, and there is no standard test protocol. This study proposes and validates a structured, reproducible method to quantify thermal power derating and verify adherence to manufacturer specifications. It also combines a controlled thermal chamber, PV emulator source, and utility grid emulator with temperature steps from 25 to 60 °C. Tests on two single-phase 8 kW inverters show that Inverter A is derated by 17.8% at nominal voltage and 9.2% at maximum voltage, with onset at 50–55 °C, despite catalog claims of no derating. Inverter B reached 33.6% at nominal voltage and 27.9% at minimum voltage, with thermal shutdown at the minimum voltage and onset at 50–60 °C. Performance differences align with cooling strategies: forced plus natural convection maintained continuous operation, whereas natural convection alone led to progressive heat buildup and instability. The findings support publishing complete derating curves at multiple MPP voltages and requiring independent tests in technical due diligence. The proposed protocol improves cross-lab comparability and narrows the gap between stated and delivered field performance.

Keywords: Photovoltaic; Inverters; Thermal; Power Derating; Standard; Laboratory Test

1. Introduction

Photovoltaic (PV) inverters are responsible for converting the power generated by PV modules, aiming to operate at the maximum power point (MPP) (Badea et al., 2025; Pereira & Silva, 2024). During operation, these devices tend to increase their internal temperature, triggering thermal management strategies when a safe limit is exceeded. One strategy involves shifting the MPP, thereby reducing the output power and avoiding overheating (Mathew & Naidu, 2024; Perin, 2016).

This reduction strategy is known as thermal power derating and is reversed once the temperature returns to a safe range, allowing the inverter to resume full power conversion. If this reduction does not occur, there is a risk of compromising the equipment's reliability and reducing its service life. On the other hand, when derating is triggered, power generation decreases. Therefore, this trade-off directly affects both lifetime and energy yield (Barreras et al., 2018; Sun et al., 2018).

In diverse engineering domains, derating has been treated as a decisive mechanism to mitigate thermal stress and preserve performance. In electrochemical storage, Ruan et al. (2023) propose a taxonomy of static and dynamic derating aimed at extending the service life of lithium-ion batteries. In the wind sector, Al-Khayat and Al-Rasheedi (2024) integrate thermal effects into generation models by combining temperature time series with turbine operational limits, which improves the reliability of forecasts and operational planning. Within the scope of reliability and lifetime of power equipment, Vernica et al. (2018) reinforce the link between thermal stress and degradation. In hybrid electric vehicles, Machacek et al. (2022) explicitly incorporate motor thermal derating into energy management through hierarchical model predictive control, ensuring thermal safety and near-optimal consumption and recovering about 70% of the performance loss observed when derating is ignored.

Despite these advances in adjacent areas, the topic remains underexplored for commercial photovoltaic inverters, although its impact on energy yield and reliability is substantial in hot regions. Technical and economic barriers persist: inverter operation is often treated as a black box, and controlled thermal testing requires costly infrastructure. Because derating directly affects energy production, it is essential that manufacturers accurately describe in their datasheets the thermal power derating behavior across the operating range.

Within the regulatory framework for photovoltaic inverters, European Standard (EN) 50524:2021 (CENELEC, 2021) defines the derating curve as an optional parameter in technical specifications. As a result, many manufacturers do

10.18086/swc.2025.03.16 Available at http://proceedings.ises.org

not include the full curve, indicating only the temperature range where power reduction should begin. Systematic evaluation of this phenomenon is also rare in the technical literature, largely due to the complexity of conducting tests under controlled temperature conditions. Testing inverters in laboratory environments already demands substantial infrastructure, and adding temperature control further increases complexity, requiring thermal chambers.

While some studies (Jeykishan Kumar et al., 2021; de Lima et al., 2023) attempted low-cost alternatives using thermal enclosures, such setups often lack precise control over temperature stabilization, compromising repeatability and standardization. To address this gap, the present study introduces a structured and reproducible methodology to evaluate thermal power derating in photovoltaic inverters under controlled laboratory conditions. The procedure defines test conditions, time intervals, and criteria consistent with datasheet specifications. Two commercial single-phase inverters (nominal power ≈ 8 kW) were tested using a stepwise temperature protocol from 25–60 °C.

The paper is organized as follows. Section 2 describes the materials and methods, detailing the thermal-derating test procedure and characterizing the inverters and the MPP voltages adopted in the tests. Next, Section 3 presents and discusses the results, organized by device and complemented by a comparative analysis that details each inverter’s thermal behavior and the indicators for the onset and magnitude of power reduction. Finally, Section 4 synthesizes the main conclusions and outlines opportunities for future work.

2. Materials and Methods

This section presents the materials and methods adopted to evaluate thermal power derating in photovoltaic inverters under controlled conditions. First, the derating test procedure is defined, including temperature steps, stabilization windows, and the selection of MPP voltage levels based on manufacturer data and the California Energy Commission (CEC) criterion. Next, the experimental setup is described, integrating a thermal chamber, a programmable PV source simulator, a programmable AC grid source, a power analyzer, an oscilloscope, and a temperature acquisition system.

Finally, the inverters under test are detailed and consistency checks between datasheet values and the voltages adopted in the protocol are reported, establishing a transparent and reproducible workflow that supports comparison across devices and laboratories

2.1. Derating Test Procedure

The inverter was installed in a thermal chamber and connected, in accordance with the manufacturer’s specifications, to a photovoltaic module emulator and to a grid source simulator under nominal conditions. The photovoltaic emulator was configured with the EN 50530:2010 standard for Electrotechnical Standardization, 2010 curve. The tests were conducted at three maximum power point voltage conditions: minimum, nominal (declared or calculated according to the CEC criterion Bower et al., 2004), and maximum.

For each voltage condition, a stepped thermal protocol was applied from 25 °C to 60 °C in 5 °C increments, with each step held for 40 minutes before proceeding. Throughout the test, the heatsink temperature, the chamber air temperature, the setpoints of the photovoltaic simulator (voltage, current, and power at the MPP), the direct current input voltage and current at the inverter, the direct current input power, and the alternating current output power were continuously recorded.

After completing the sequence at the minimum voltage, the procedure was repeated at the nominal voltage and then at the maximum voltage. Finally, input and output power curves and thermal profiles were derived, identifying the onset temperature of power reduction, the maximum derating, and the corresponding heatsink temperature.

2.2. Derating Test Procedure

The experimental arrangement for advanced thermal derating tests is presented in Figures 1 and 2. Tests were conducted in a bench comprising a thermal chamber, a programmable photovoltaic simulator (IT6018C-1500-40), a programmable AC grid source (IT7930-350-180), a power analyzer, an oscilloscope for transient and waveform analysis, and a temperature acquisition system. The inverter under test was installed inside the chamber, with ambient temperature controlled in discrete steps from 25 to 60 °C under continuous stability verification.

The direct current side was supplied by a photovoltaic simulator configured with the EN 50530 standard curve, with the operating point set to the three MPP voltage conditions: minimum, nominal declared or calculated according to the CEC criterion, and maximum. The alternating current side was connected to a programmable AC source adjusted to the nominal test conditions, ensuring constant voltage and frequency throughout the thermal sequence.

Electrical quantities were measured simultaneously on the DC and AC sides using an LMG-671 power analyzer, with sampling sufficient to capture variations within each thermal step, while an oscilloscope monitored possible transient events such as internal switching, momentary power dips, and restarts. Temperature was tracked by thermocouples sensors on the inverter heatsink and by air sensors inside the chamber, acquired by a GL240 multi-channel logger, enabling direct correlation between converted power and thermal profile. The system includes isolation, protection, and interlocks between DC and AC for safe operation.

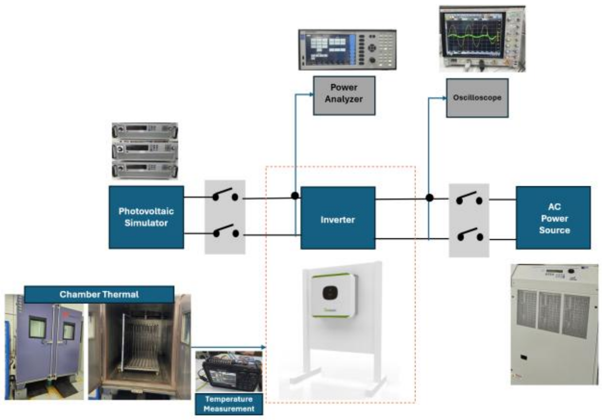

Figure 1: Schematic diagram of the experimental setup used for thermal derating evaluation.

Figure 2: Experimental setup used during the thermal derating tests.

2.3. Inverters Test

Two single-phase inverters, labeled A (8.2 kW) and B (8.0 kW), both rated for 220 V, were tested under power and voltage conditions taken from their datasheet. Inverter A declares minimum, nominal, and maximum MPP voltages of 240 V, 710 V, and 800 V, respectively. According to the CEC criterion (Bower2004), the nominal MPP voltage must satisfy:

$$V_{min} + 0.25(V_{max} - V_{min}) \leq V_{nom} \leq V_{min} + 0.75(V_{max} - V_{min}) \text{ (eq. 1)}$$

Since the declared nominal value does not fall within this range, a new nominal voltage was calculated, resulting in four tested voltage levels. Inverter A features both natural and forced convection cooling systems. Inverter B declares a minimum voltage of 90 V, but 200 V was adopted in the test, as it represents the minimum voltage required to support nominal power without exceeding the current limit (13 A). The nominal voltage was not provided, so it was calculated based on the same CEC (Bower et al., 2004) criterion. The declared maximum MPP voltage is 520 V, which was corrected to 440 V by applying the standard's recommendation of using 80% of the open-circuit voltage. Inverter B uses only natural convection for cooling.

The methodology adopted in this study requires verifying whether the inverter's operating characteristics are compatible with the test protocol, particularly regarding the input voltage levels. For that purpose, Table 1 presents a comparison between the datasheet values and the values adopted during the tests. This comparison ensures that the test conditions comply with the criteria established for minimum, nominal, and maximum MPP voltages.

Table 1: Datasheet information and test values for photovoltaic inverters.

Specification	Inverter A (8.2 kW)		Inverter B (8.0 kW)	
	Datasheet	Test Value	Datasheet	Test Value
Nominal Power [kW]	8.2	8.2	8.0	8.0
Nominal AC Voltage (Vac) [V]	220	220	220	220
Min. MPP Voltage (VMPP,min) [V]	270	270	90	200
Nom. MPP Voltage (datasheet) (VMPP,nom,ds) [V]	710	710	Not informed	--
Nom. MPP Voltage (calculated) (VMPP,nom,calc)[V]	--	535	--	360
Max. MPP Voltage (VMPP,max) [V]	800	800	520	440
Max. DC Input Voltage (Vdc,max) [V]	1000	1000	550	550
Max. Input Current [A]	18.0	18.0	13.0	13.0

3. Results and Discussion

This section presents the results of the thermal derating tests performed on two commercial photovoltaic inverters with nominal powers of 8.2 kW (Inverter A) and 8.0 kW (Inverter B), respectively. These devices were selected to allow a comparative evaluation of their performance under controlled high-temperature conditions. Based on the predefined voltage conditions and the standardized procedure, the methodology was applied to assess the derating behavior of each inverter across different DC voltage levels.

3.1. Inverter A

According to the manufacturer of Inverter A, when operating at the minimum MPP voltage (240 V), the inverter is expected to maintain maximum output power up to 40 °C. Above this temperature, a gradual derating is specified, reaching a minimum output power of approximately 6,200 W at 50 °C. At the nominal (710 V) and maximum (800 V) MPP voltages, no derating is indicated, which implies that the inverter should maintain nominal performance throughout the operating temperature range.

However, the experimental results revealed significant deviations from the expected behavior. A comparison between datasheet information and measured results for Inverter A, shown in Figures 3 to 6, highlights these differences. The curves depict the inverter's dynamic response throughout the temperature steps: green and orange lines denote DC and AC power; a black dashed line marks the MPP, fixed at 8,200 W for Inverter A; a blue line traces the air temperature inside the thermal chamber; a gray dashed line indicates the control temperature set for each step; and a purple line shows the heatsink temperature. Taken together, these curves reveal both the onset and progression of derating, as well as the system's thermal response over time.

At 240 V, the minimum voltage as shown in Figure 3, the datasheet indicates a maximum derating of 24.39% beginning at 40 °C, reaching a minimum output power of 6,200 W at 50 °C. The measurements, however, revealed a more pronounced derating, with a minimum output power of 5,709.81 W and a corresponding maximum derating of 25.67%. The onset temperature for derating was also higher, 50 °C rather than 40 °C, suggesting that under controlled conditions the unit sustains nominal operation slightly beyond the manufacturer's stated threshold.

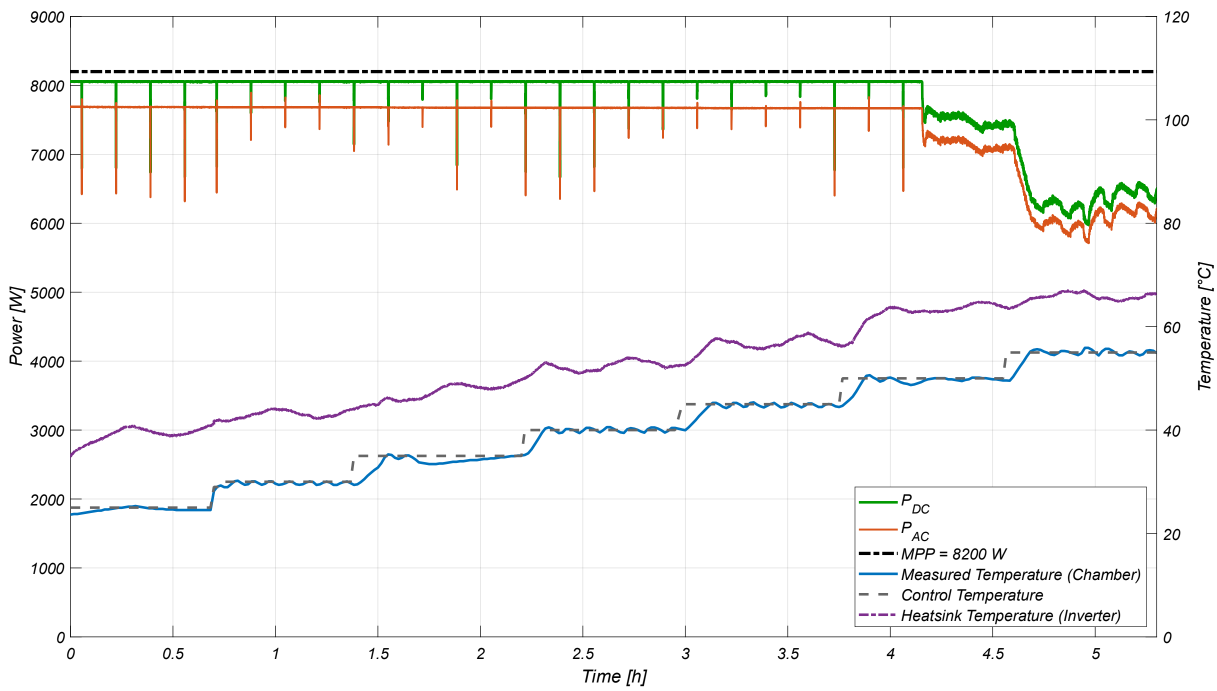

Figure 3: Derating behavior of inverter A at 240 V.

At 710 V, the nominal voltage declared in the datasheet and shown in Figure 4, no derating behavior was specified by the manufacturer, and stable operation across the temperature range was expected. Nevertheless, the measurements indicated a significant reduction, with a minimum output power of 6,514.51 W and a maximum derating of 17.78%. This divergence highlights that, even when datasheets omit detailed behavior at nominal voltage, thermal stress during operation can still cause noticeable performance degradation.

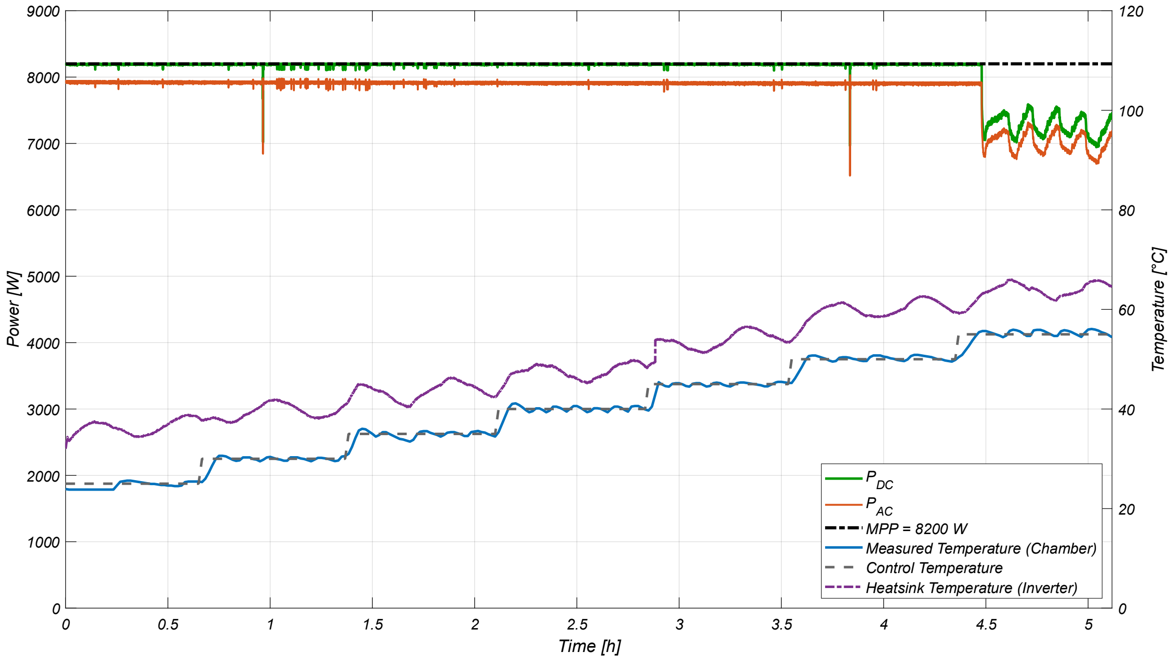

Figure 4: Derating behavior of inverter A at 710 V.

At 800 V, the maximum MPP voltage and shown in Figure 5, the datasheet indicates no derating. Experimentally, a derating of 9.17 percent was observed, with output power dropping to 7,183.33 W at the highest tested temperatures. Short generation interruptions were also observed during the test, corresponding to inverter shutdowns of approximately one minute each. Because these events were not caused by thermal limitation, they were excluded from the performance analysis.

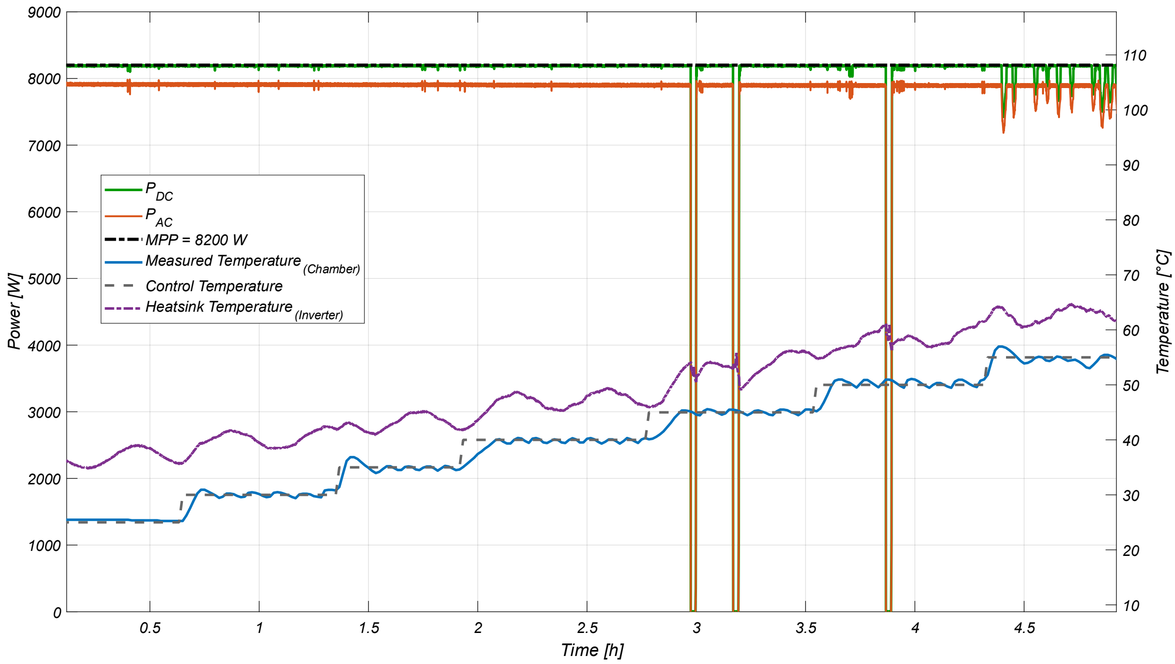

Figure 5: Derating behavior of Inverter A at 800 V.

Overall, the measured results show that while the datasheet generally captures the expected trends at minimum voltages, it underestimates or omits important derating behavior at nominal and maximum operating voltages. These findings emphasize the relevance of independent laboratory evaluations to accurately characterize inverter performance under real-world thermal conditions.

As shown in Figure 6, the derating behavior of Inverter A at the calculated nominal voltage (535 V) resulted in a power reduction of 13.89%, with the lowest output power measured at 6804.77 W. This point was selected as an intermediate value to better cover the full MPP operating range, based on international standards. Interestingly, the power reduction observed at 710 V was greater, reaching 17.78%, even though 535 V involves higher input currents, which would theoretically impose greater thermal stress. This result diverges from the initial assumption that lower voltages would necessarily lead to more severe derating.

On the other hand, the previous tests, applying the same methodology, produced results in line with the original hypothesis, that is a greater reduction at 535 V than at 710 V. This discrepancy reinforces the importance of experimentally evaluating the entire MPP voltage range, since different inverter designs may present different thermal responses under similar conditions.

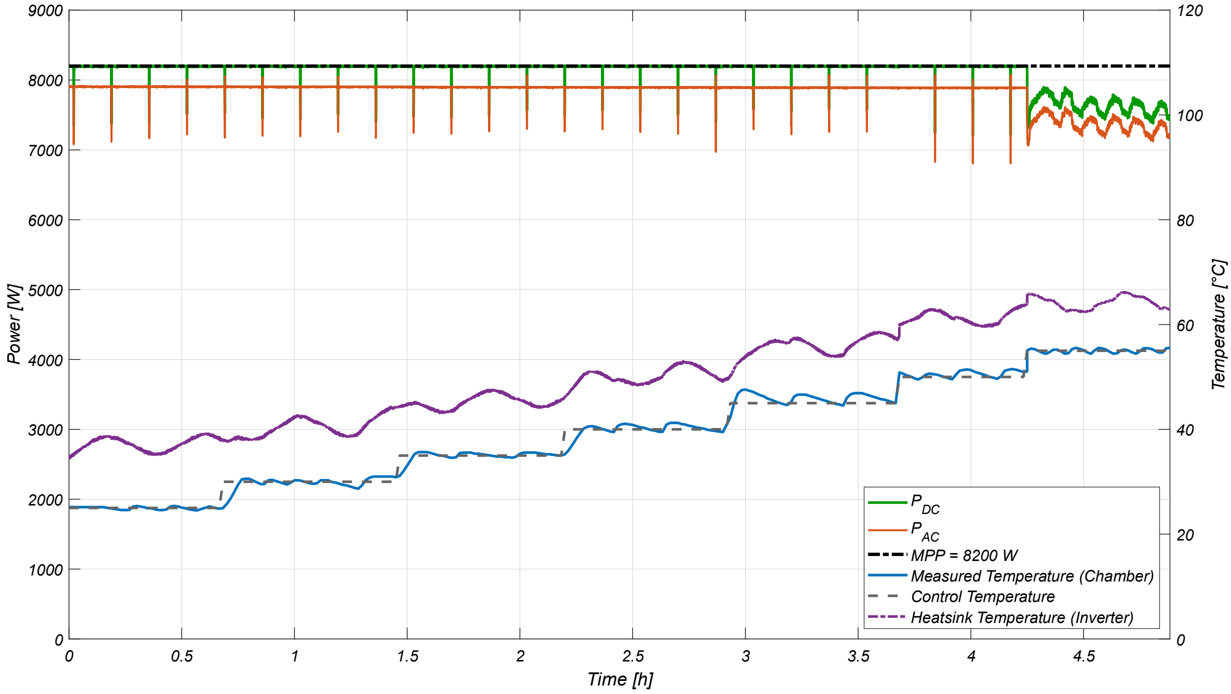

Figure 6: Derating behavior of inverter A at 535 V.

The key findings regarding the thermal derating behavior of Inverter A are summarized in Table 2. This table compares the manufacturer's datasheet information with the measured results for each tested DC voltage condition. It highlights differences in the onset temperature for derating, the minimum output power reached, and the corresponding maximum derating percentages. These comparisons provide a comprehensive view of the inverter's real thermal performance and demonstrate the deviations from the specifications provided by the manufacturer.

Table 2: Comparison between datasheet and measured derating data for Inverter A at different DC voltages.

Parameter	Datasheet			Measured			
	240 V (min)	710 V (nominal)	800 V (max)	240 V (min)	535 V (calculated)	710 V (nominal)	800 V (max)
Start temperature of derating [°C]	40	--	--	50	55	55	55
Temperature at maximum derating [°C]	50	--	--	55	55	55	55
Minimum power during derating [W]	6200	--	--	5709.81	6804.77	6514.51	7183.33
Maximum derating [%]	24.39	--	--	25.67	13.89	17.78	9.17

3.2. Inverter B

The manufacturer's datasheet for Inverter B does not provide a detailed thermal derating curve. Instead, it only states that a reduction in power may occur when the equipment operates above 45°C. However, it does not specify the magnitude of the derating, the expected minimum output power, or the temperatures at which the derating would stabilize.

Experimental results revealed the detailed thermal derating behavior of Inverter B under controlled laboratory conditions. The plotted curves in Figures 7 to 9 depict the inverter response at each test step. In these graphs, the green and orange lines represent the DC and AC power, respectively, while the dashed black line corresponds to the defined MPP, set at 8000 W for Inverter B. The blue line shows the temperature measured in the chamber, the gray dashed line represents the control temperature at each step, and the purple line indicates the temperature measured at the inverter heatsink. These visualizations provide insight into the onset of derating, the stability of power delivery, and the progressive accumulation of heat across different voltage conditions.

At 200 V, the minimum voltage as shown in Figure 7, derating began at 50 °C. At 55 °C the reduction intensified, lowering power to about 5,500 W and causing the heatsink temperature to drop from roughly 100 °C to 92 °C. As the temperature decreased, nominal operation was briefly resumed, but the internal temperature rose again, triggering a new derating phase followed by a complete shutdown. The minimum AC power recorded before shutdown was 5,456.74 W, corresponding to a maximum power derate of 27.91%.

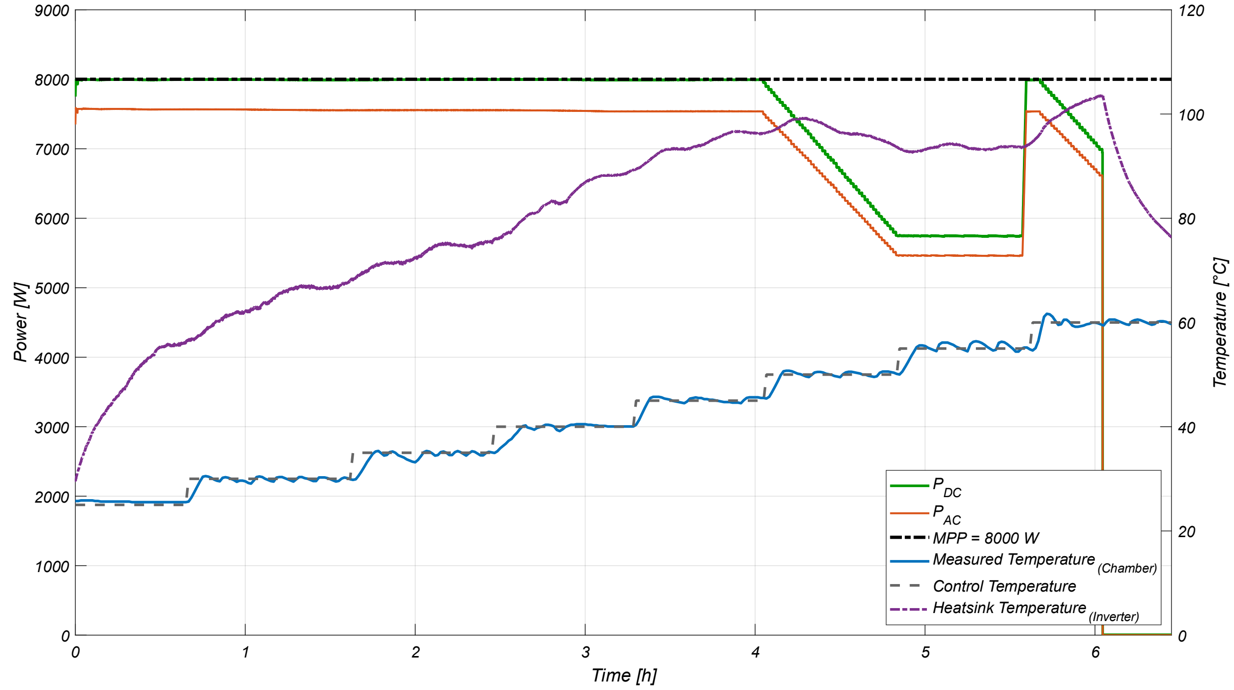

Figure 7: Derating behavior of inverter B at 200 V.

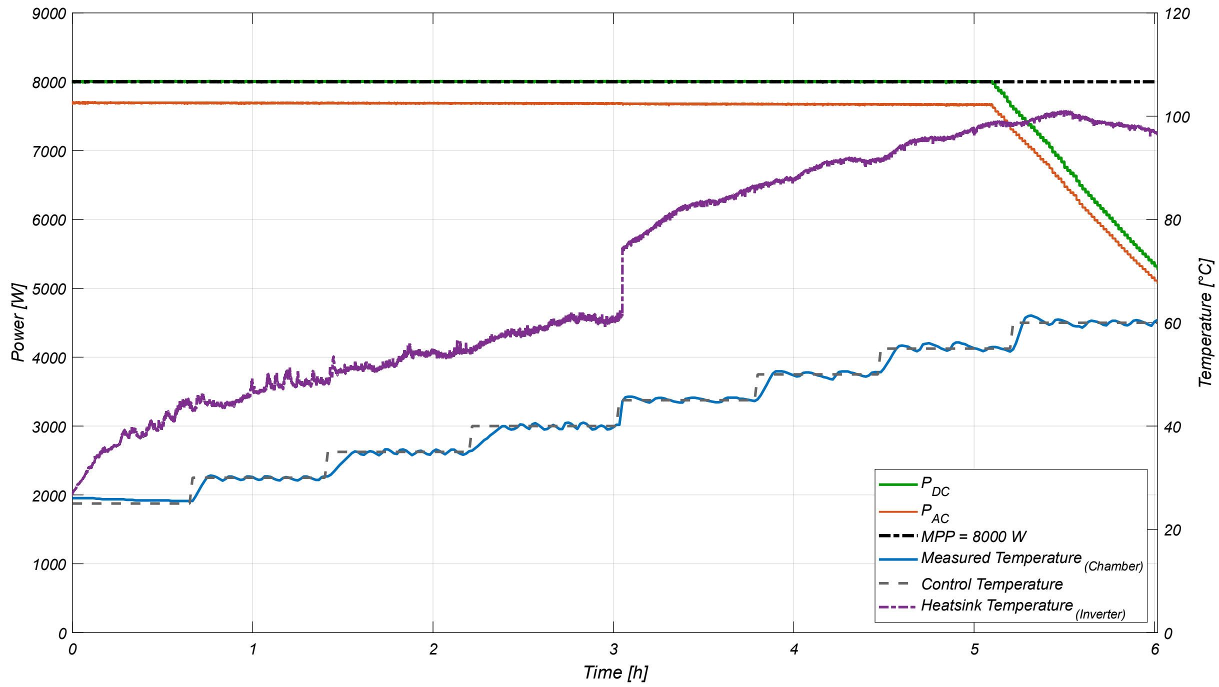

Figure 8: Derating behavior of inverter B at 360 V.

At 360 V, the calculated nominal voltage as shown in Figure 8, derating began at 55 °C and continued to 60 °C, yielding a more pronounced reduction. The minimum AC output power recorded was 5,111.17 W, corresponding to a maximum derating of 33.57%. During this test the thermal chamber experienced a temporary freeze; after restart, the heatsink temperature rose briefly. This incident did not affect the results, as no power reduction was observed during that interval.

At 440 V, the maximum voltage as shown in Figure 9, derating was observed only at the highest temperature levels, with a minimum AC output power of 6,418.97 W and a corresponding maximum derating of 16.87%. The inverter remained stable up to approximately 55 °C, after which the power reduction became significant. During the test at maximum voltage, the thermal chamber required a restart; this event caused a brief rise in heatsink temperature, yet no derating was recorded and the inverter maintained stable output throughout the interval.

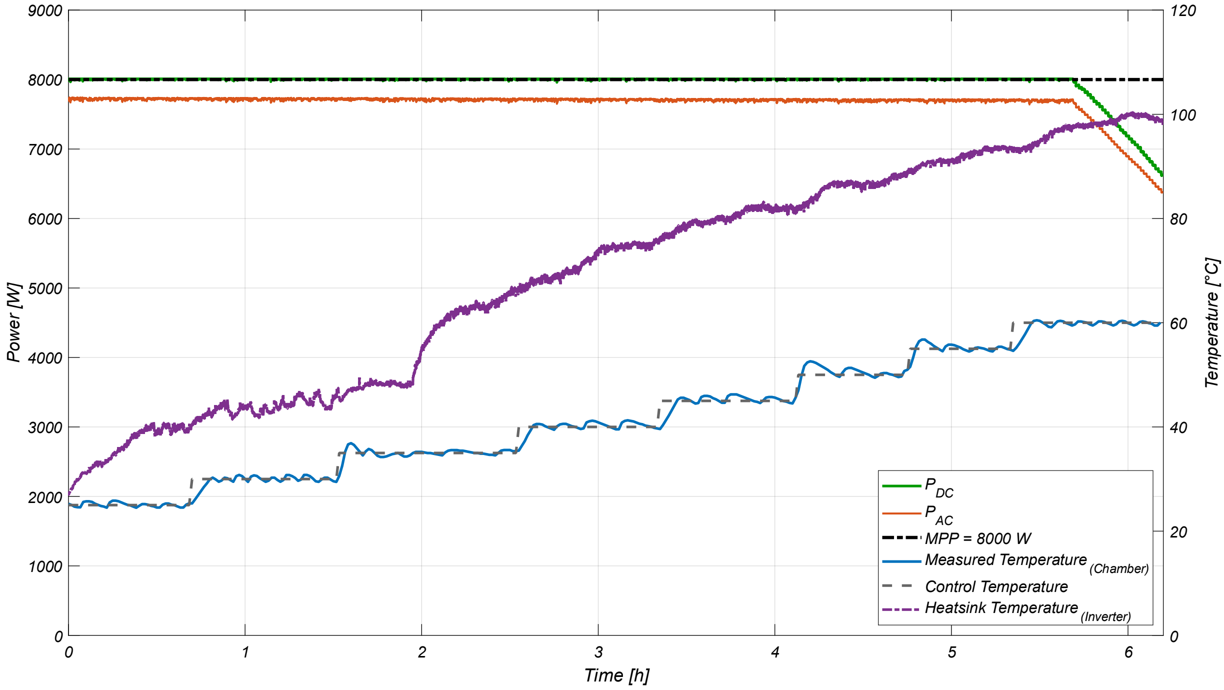

Figure 9: Derating behavior of Inverter B at 440 V.

The summary of the measured derating parameters for each voltage is presented in Table 3. Although the datasheet does not contain quantitative information for direct comparison, the measured results allow a clear assessment of the inverter behavior under temperatures above 25°C. As mentioned, an asterisk (*) is used in the table to indicate that the minimum output power at 200 V was recorded immediately before the inverter shutdown caused by thermal protection.

Table 3: Comparison between datasheet and measured derating data for Inverter B at different DC voltages.

Parameter	Datasheet			Measured		
	200 V	360 V	440 V	200 V	360 V	440 V
Start temperature of derating [°C]	45	45	45	50	55	60
Temperature at maximum derating [°C]	--	--	--	60	60	60
Minimum power during derating [W]	--	--	--	5456.74*	5111.17	6418.97
Maximum derating [%]	--	--	--	27.91*	33.57	16.87

* Value measured immediately before thermal shutdown.

3.3. Comparative analysis: Inverter A and Inverter B

The thermal derating behavior of the two inverters, when evaluated under their datasheet-specified MPP voltage levels (minimum, nominal, and maximum), reveals significant differences in performance and thermal resilience.

To begin with, the datasheet of Inverter A defines its maximum operating temperature as 55°C, while Inverter B allows operation up to 60°C. This distinction already suggests a higher declared thermal tolerance for Inverter B. However, the actual performance under thermal stress shows that datasheet limits may not reflect the inverter's true operational robustness. Table 4 shows that presents the comparative values.

At the nominal voltage, Inverter A showed a power reduction of 17.78%, falling from 7921.22 W to 6514.51 W. Meanwhile, Inverter B displayed a more pronounced derating of 33.60%, with its power decreasing from 7694.19 W to 5111.17 W. This result reveals a clear advantage in thermal stability for Inverter A, which managed to maintain a higher output level under the same thermal stress.

Table 4: Comparison of measured derating data between Inverter A and Inverter B at datasheet voltage levels.

Parameter	Inverter A			Inverter B		
	240 V (min)	710 V (nominal)	800 V (max)	200 V (min)	360 V (nominal)	440 V (max)
Start temperature of derating [°C]	50	55	55	50	55	60
Temperature at maximum derating [°C]	55	55	55	60	60	60
Minimum power during derating [W]	5709.81	6514.51	7183.33	5456.74*	5111.17	6418.97
Maximum derating [%]	25.67	17.78	9.17	29.92	33.60	16.81

* Value measured immediately before thermal shutdown.

At the maximum voltage, Inverter A exhibited the lowest derating among the three tested voltages, 9.17%, with output dropping to 7183.33 W. Inverter B, on the other hand, reduced its power from 7721.94 W to 6418.97 W, resulting in a derating of 16.83%. Although both inverters maintained operation during this phase, Inverter A again demonstrated superior thermal performance.

These findings suggest that, even though Inverter B declares a higher maximum operating temperature, its thermal behavior under laboratory-controlled stress conditions resulted in deeper power losses and operational instability. Inverter A, despite a lower declared thermal limit, maintained more consistent performance and did not shut down at any point during the test.

This may be explained by the cooling mechanisms used: Inverter A combines forced and natural convection, which results in fluctuating dissipator temperatures and a less linear thermal profile. In contrast, Inverter B uses only passive cooling, which contributes to the more stable but progressively higher dissipator temperatures observed. This difference is highlighted in Table 5, which compares the maximum dissipator temperatures recorded during each step of the derating tests for both inverters.

Table 5: Maximum heat sink temperature [°C] recorded at each control step for Inverters A and B at comparable DC voltage levels.

Step Temp. [°C]	Minimum Voltage		Nominal Voltage		Maximum Voltage	
	A (240 V)	B (200 V)	A (710 V)	B (360 V)	A (800 V)	B (440 V)
25	40.90	56.20	38.00	44.80	39.00	36.00
30	44.00	68.10	41.80	50.70	42.30	43.77
35	49.00	75.00	46.30	56.30	45.20	55.58
40	53.00	89.00	49.70	61.70	49.30	71.66
45	58.00	96.00	56.50	86.20	56.20	80.24
50	64.00	99.20	62.60	91.90	61.60	86.20
55	66.00	94.30	65.90	99.00	65.20	91.81
60	--	103.50	--	100.20	--	97.35

The heatsink temperatures recorded during each control step reveal a clear contrast between the thermal responses of the two inverters. For example, at the 40°C control step, inverter A operating at 240V recorded a maximum heatsink temperature of 53.90°C, while Inverter B at 200V reached 89.30°C, a difference of more than 35°C under the same environmental conditions. This pattern persists across all voltages and temperature levels tested. While inverter A exhibits greater fluctuation between steps, Inverter B exhibits a more gradual and sustained increase.

These discrepancies highlight the distinct thermal behaviors of each design and how the inverter architecture impacts heat buildup throughout the power derating process. In these cases, it can be seen that Inverter A, operating at lower heatsink temperatures, performed better overall during testing. Therefore, it is important to evaluate thermal profiles when interpreting inverter performance under elevated temperature conditions.

4. Conclusions and Future Work

This work presented a structured and reproducible methodology to quantify temperature-induced power reduction in photovoltaic inverters under controlled conditions. It addresses the study's central question of how to measure, compare, and report this reduction in a standardized manner and whether it adheres to catalog information. Applied to two single-phase inverters of about 8 kW, the approach employs temperature steps from 25 °C to 60 °C, stabilization windows, and careful selection of MPP voltages at the minimum, the nominal declared or calculated, and the maximum values, yielding comparable metrics across units.

As main results, it was found that Inverter A, despite declaring no power reduction at nominal and maximum voltages, showed measurable drops of about 17.8% at 710 V and 9.2% at 800 V, with the onset of reduction between 50 and 55 °C. Inverter B, whose catalog provides no detailed curve and only indicates reduction above 45 °C, exhibited deeper losses, notably about 33.6% at 360 V, and shut down due to thermal protection at the minimum voltage condition; the onset of reduction occurred between 50 and 60 °C depending on voltage. The performance contrast is associated with cooling strategies: Inverter A, using forced and natural convection, maintained continuous operation, whereas Inverter B, relying only on natural convection, progressively accumulated heat, resulting in operational instability. These findings reveal gaps between catalog declarations and observations from independent tests, especially in voltage ranges where many manufacturers do not report complete curves.

On the methodological front, the study advances by defining a replicable protocol with thermal steps, stabilization times, voltage selection, and criteria for onset and maximum reduction, by proposing a set of metrics that supports comparative analyses across laboratories and manufacturers, and by integrating the thermal assessment into the regulatory context in which EN 50524 treats the reduction curve as optional information, a fact that in practice hinders technical auditing and equipment comparison. The results show that thermal losses at high temperatures and at different MPP voltage points are not negligible. These losses should be incorporated into energy production and risk models, directly impacting inverter selection for hot climates, ventilation and installation criteria, design margins, and bankability assessments.

As a recommendation, manufacturers should report complete power reduction curves as a function of temperature at multiple MPP voltages, so that performance becomes transparent and uncertainties between catalog values and field delivery are reduced.

Future work includes expanding the sample to include three phase inverters and higher power ratings with diverse thermal architectures; studying dynamic thermal profiles with daily cycling, airflow variation, and installation conditions; and determining the optimal balance between performance and thermal management of the equipment.

5. Acknowledgments

This study was financed by TotalEnergies through the R&D incentive program of the Brazilian National Agency of Petroleum, Natural Gas and Biofuels in partnership with CEPETRO and FEEC at UNICAMP.

6. References

Al-Khayat, M., Al-Rasheedi, M., 2024. A new method for estimating the annual energy production of wind turbines in hot environments. Renewable and Sustainable Energy Reviews 195, 114343. https://doi.org/10.1016/j.rser.2024.114343

Badea, A.-M., Manaila-Maximean, D., Fara, L., Craciunescu, D., 2025. Maximizing solar photovoltaic energy efficiency: MPPT techniques investigation based on shading effects. Solar Energy 285, 113082. https://doi.org/10.1016/j.solener.2024.113082

Barreras, J.V., Raj, T., Howey, D.A., 2018. Derating strategies for lithium-ion batteries in electric vehicles. In: IECON 2018 – 44th Annual Conference of the IEEE Industrial Electronics Society, 4956–4961. https://doi.org/10.1109/IECON.2018.8592901

Bower, W., Whitaker, C., Erdman, W., Behnke, M., Fitzgerald, M., 2004. Performance test protocol for evaluating inverters used in grid-connected photovoltaic systems. Sandia National Laboratories, Albuquerque, NM.

CENELEC (European Committee for Electrotechnical Standardization), 2010. EN 50530:2010 — Overall efficiency of grid-connected photovoltaic inverters. CENELEC.

CENELEC (European Committee for Electrotechnical Standardization), 2021. EN 50524:2021 — Data sheet for photovoltaic inverters. CENELEC.

de Lima, G.P., Ribeiro, A.C., Lemos, F.V.E., Silveira, J.P.C., Barros, T.A.S., Villalva, M.G., 2023. Comparing temperature derating test in the laboratory with commercial photovoltaic inverter datasheet. In: 2023 IEEE 8th Southern Power Electronics Conference and 17th Brazilian Power Electronics Conference (SPEC/COBEP), 1–7. https://doi.org/10.1109/SPEC56436.2023.10407835

Jeykishan Kumar, K., Sudhir Kumar, R., Bhattacharjee, T., 2021. Alternate method for evaluating power-temperature derating characteristics of grid-tie solar photovoltaic inverter. Sādhanā 46(3), 1–13.

Machacek, D.T., Barhoumi, K., Ritzmann, J.M., Huber, T., Onder, C.H., 2022. Multi-level model predictive control for the energy management of hybrid electric vehicles including thermal derating. IEEE Transactions on Vehicular Technology 71(10), 10400–10414. https://doi.org/10.1109/TVT.2022.3183866

Mathew, D., Naidu, R.C., 2024. A review on single-phase boost inverter technology for low-power grid-integrated solar PV applications. Ain Shams Engineering Journal 15(2), 102365. https://doi.org/10.1016/j.asej.2023.102365

Pereira, F., Silva, C., 2024. Machine learning for monitoring and classification in inverters from solar photovoltaic energy plants. Solar Compass 9, 100066. https://doi.org/10.1016/j.solcom.2023.100066

Perin, A.L., 2016. Análise da influência de diferentes estratégias de arrefecimento no desempenho e durabilidade de inversores de sistemas fotovoltaicos conectados à rede. [Dissertação/Tese, completar instituição e cidade].

Ruan, H., Barreras, J.V., Engström, T., Merla, Y., Millar, R., Wu, B., 2023. Lithium-ion battery lifetime extension: A review of derating methods. Journal of Power Sources 563, 232805. https://doi.org/10.1016/j.jpowsour.2023.232805

Sun, Y., Saxena, S., Pecht, M., 2018. Derating guidelines for lithium-ion batteries. Energies 11(12), 3362. https://doi.org/10.3390/en11123362

Vernica, I., Ma, K., Blaabjerg, F., 2018. Optimal derating strategy of power electronics converter for maximum wind energy production with lifetime information of power devices. IEEE Journal of Emerging and Selected Topics in Power Electronics 6(1), 267–276. https://doi.org/10.1109/JESTPE.2017.274571